LEFT VENTRICULAR STRESSES IN THE INTACT HUMAN HEART

I. MIRSKY

From the Department of Medicine, Division of Mathematical Biology, Harvard Medical School and Peter Bent Brigham Hospital, Boston, Massachusetts 02115

ABSTRACT A set of stress differential equations of equilibrium is presented for a thick prolate spheroid which is the assumed shape for the left ventricle. An analysis for the stresses in the ventricular wall indicates that maximum stresses occur at the inner layers and decrease to a minimum at the epicardial surface, a result that is partially validated by experiment. Simple expressions are available for the evaluation of maximum stresses which occur at the equator and are suitable for small laboratory-oriented digital computers employed in the clinical evaluation of patient status. The surprising result is that Laplace's law yields practical values for mean stresses in thick-walled ventricles.

INTRODUCTION

Many diagnostic techniques are available to the clinical cardiologist and in many cases the diagnosis of a particular cardiovascular disease is straightforward. However, quite often these diagnostic tools are unable to detect severe and potentially operable degrees of the disease, as for example when aortic stenosis and aortic insufficiency exist simultaneously. In order to provide the clinician with more sophisticated diagnostic techniques, one must gain a better understanding of the mechanics and performance of the myocardium. This requires an accurate analysis of the forces and stresses developed in the wall of the left ventricle throughout the cardiac cycle.

Most physiologists interested in calculating wall forces in the left ventricle have applied the law of Laplace which relates the pressure difference across a membrane surface to its curvature and surface tension. Wood (1892) was the first to apply the law for the evaluation of wall tension in the heart and later, Burch et al. (1952) and Burton (1957) demonstrated via this law, the importance of size and shape of the ventricle to its performance. Assuming an ellipsoidal geometry, Sandler and Dodge (1963) analyzed the stresses in the left ventricle and for the special cases of the cylinder and the sphere compared Laplace's law with the exact solutions.

More recently, thick shell theories have been developed by Ghista and Sandler (1967) and Wong and Rautaharju (1968). Their analyses yield nonlinear stress dis-

tributions through the wall thickness, a result which cannot be predicted by Laplace's law. However, their assumptions with regard to the deformation behavior of the left ventricle are restrctive. A theory, to be valid for thick shell structures, must include the effects of transverse normal stress (radial stress) and transverse shear deformation which always accompanies bending stresses. These effects, which are significant for the left ventricle, are entirely neglected in the development of Laplace's law.

In this investigation, a system of differential equations is presented for the stress equilibrium in the left ventricular wall assuming an ellipsoidal geometry. These equations have been derived from the exact three dimensional equations of elasticity employing the method of the calculus of variations. An analysis for the left ventricular stresses is based on a numerical integration and asymptotic method of solution to these differential equations. Geometrical data employed in the evaluation of the stresses was obtained from biplane angiocardiography.

Numerical results indicate that maximum stresses occur in the circumferential direction on the endocardial surface at the equator of the ellipsoid. These maximum stresses occur either prior to, or at the time of, peak left ventricular pressure. The nonlinear stress distributions through the wall thickness are validated in part by the experimental studies of Laszt and Müller (1958) and Kreuzer and Schoeppe (1963). The theory is in fair agreement with the experimental data during diastole, however there are discrepancies for the systolic phase. This may imply that the assumptions of isotropy and homogeneity of the wall material are reasonable for a heart in a passive state but that anisotropy and nonhomogeneity may be important factors to consider in the contractile state. Comparisons of results from the present theory are made with Laplace's law for the cases of a sphere and the prolate spheroid. The striking result is that Laplace's law predicts mean stress values in the ellipsoid to within 15% of midwall stresses obtained on the basis of the present theory for relatively thick shells. For the sphere the discrepancy is below 5%.

Although the present theory may not be quite adequate for the systolic phase, recent results obtained by Hugenholtz et al. (1968) utilizing this thick-walled theory have predicted accurately myocardial performance for 18 patients with primary myocardial, valvular, or congenital heart disease. Until a theory is developed which includes both the effects of anisotropy and nonhomogeneity, Laplace's law remains a useful tool for predicting mean wall stresses in the myocardium unless one is more concerned with localized stresses.

Basic Assumptions

In the development of the mathematical model for the mechanics of the myocardium, the following assumptions are made:

(*a*) The laws of elasticity as applied to nonliving bodies also apply to heart muscle tissue. In particular, the superposition principle and generalized Hooke's law is valid for the pressure loading.

(*b*) The myocardium is a freely deforming body composed of an isotropic and homogeneous elastic material. Furthermore, since the muscle volume remains essentially constant (except in the case of hypertrophy), one may assume that the material is incompressible for which the Poisson's ratio $\nu = 0.5$.

(c) Throughout the cardiac cycle the geometry of the ventricle is approximated by a prolate spheroid of uniform wall thickness.

(*d*) The problem is considered to be quasi-static i.e., instantaneous measurements of geometry and left ventricular pressure are employed in a static analysis for the evaluation of instantaneous stresses throughout the cardiac cycle.

(*e*) Ventricular wall stresses and deformations are independent of the circumferential coordinate and are due to the left ventricular pressure only.

These assumptions are also made in the development of Laplace's law, however in the present theory the effects of transverse normal stress (radial stress) and transverse shear are included.

It is quite apparent that, for the particular case of the left ventricle, these assumptions are rather restrictive. Certainly in the case of cardiac motion one deals with large deformations to which the linear theory does not apply. However, one may argue that although deformations are large over the complete cardiac cycle the quasi-static analysis is performed over short intervals of time for which the deformations are small. The effects of anisotropy and nonhomogeneity are presently being studied by the author and the results of this investigation will enable one to assess the validity of assumption (*b*). A more detailed discussion of these assumptions is presented later in the analysis.

Geometrical Relations and Displacement Functions

With reference to the cylindrical coordinate system (r, θ, z), we may represent the middle surface of a closed ellipsoidal shell of revolution in the parametric form

$$r = b \sin \xi, \qquad z = -a \cos \xi \qquad 0 \leqq \xi \leqq \pi \tag{1}$$

where a and b are, respectively, the semimajor and semiminor axes of the elliptical cross-section of the middle surface. The coordinate ξ represents the eccentric angle of the ellipse. If φ denotes the inclination of the tangent to the meridian at the point P of the shell as shown in Fig. 1. then

$$r' = \alpha \cos \varphi \qquad z' = \alpha \sin \varphi \tag{2}$$

where

$$\alpha^2 = (r')^2 + (z')^2 = a^2 \sin^2 \xi + b^2 \cos^2 \xi \tag{3}$$

and primes denote differentiation with respect to ξ. In terms of these quantities the two principal radii of curvature of the middle surface are denoted by

$$R_\xi = \alpha^3/ab, \qquad R_\theta = \alpha b/a. \tag{4}$$

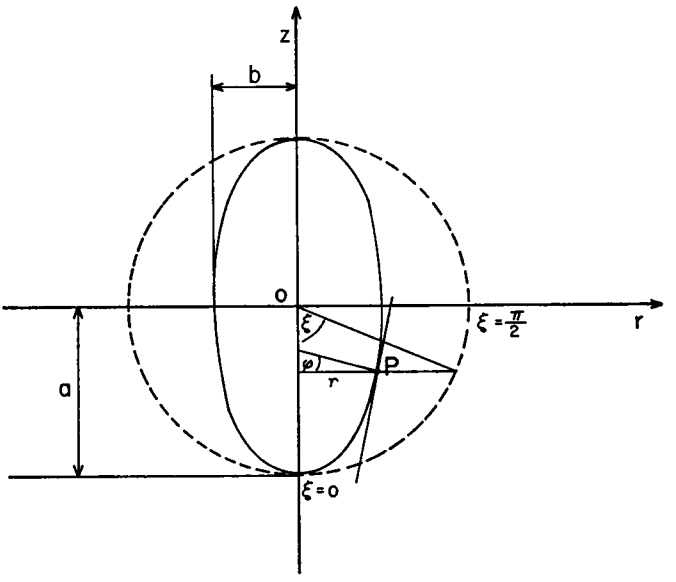

FIGURE 1 Coordinate system.

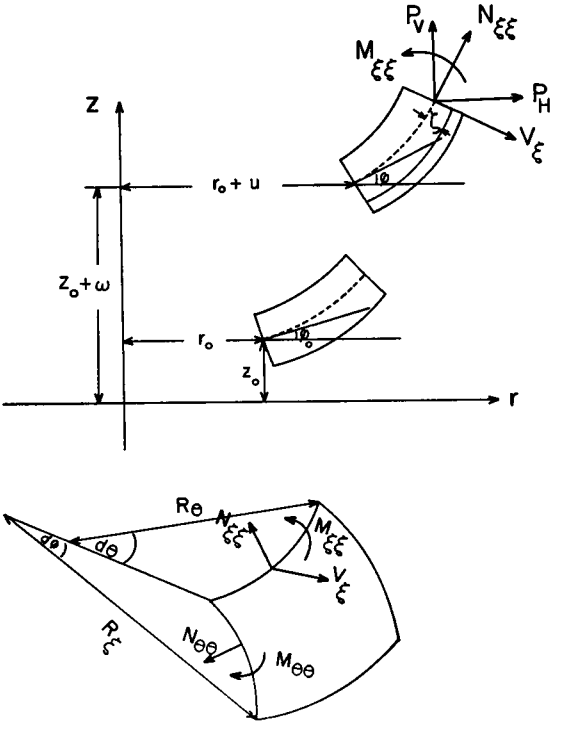

FIGURE 2 Element of shell in deformed and undeformed state and indicated stress and moment resultants.

Hence at the apex ($\xi = 0$), $R_\xi = R_\theta = b^2/a$, and at the equator ($\xi = \pi/2$), $R_\xi = a^2/b$, and $R_\theta = b$.

In the development of a shell theory one assumes approximate expressions for the displacement components. For the present theory these displacements take the form

$$\begin{aligned} U &= u_\xi + \zeta\beta \\ W &= w_\zeta + \zeta w_1 + \tfrac{1}{2}\zeta^2 w_2 \end{aligned} \tag{5}$$

where U and W are, respectively, the displacement components in the meridional and normal directions, β is the change of slope of the normal to the middle surface and w_1, w_2 are the contributions to the transverse normal or radial strain. Furthermore, ζ is the distance measured along the outward normal to the middle surface as shown in Fig. 2. It is of interest to note that in the membrane theory, upon which Laplace's law is based, the displacement components are assumed to be

$$U = u_\xi, \qquad W = w_\zeta \tag{6}$$

which in the present analysis are the displacement components at the middle surface.

Shell Equations of Equilibrium

The derivation of an approximate system of equations of equilibrium and stress-strain relations is obtained by the application of a variational theorem due to Reissner (1950). This involves a rather lengthy and tedious analysis which will not be presented here. For a more detailed discussion of the method one is referred to the work of Naghdi (1957) and Mirsky (1964), (1967).

The stress differential equations of equilibrium are given by

$$(rN_{\xi\xi})' - r'N_{\theta\theta} + (\alpha r/R_\xi)V_\xi = 0 \tag{7}$$

$$(rV_\xi)' + \alpha r p H^- = \alpha r(N_{\xi\xi}/R_\xi + N_{\theta\theta}/R_\theta) \tag{8}$$

$$(rM_{\xi\xi})' - r'M_{\theta\theta} - \alpha r V_\xi = 0 \tag{9}$$

where the stress resultants $N_{\xi\xi}$, $N_{\theta\theta}$, moment resultants $M_{\xi\xi}$, $M_{\theta\theta}$, and transverse shear force V_ξ are depicted in Fig. 2. Furthermore, p denotes the left ventricular pressure, h the uniform wall thickness, and H^- is given by

$$H^- = 1 - (h/2)(1/R_\xi + 1/R_\theta) + h^2/4R_\xi R_\theta . \tag{10}$$

For very thin shells, the transverse shear force $V_\xi = 0$, $H^- \sim 1$ and equation 8 simplifies to

$$N_{\xi\xi}/R_\xi + N_{\theta\theta}/R_\theta = p \tag{11}$$

which is the generalized form of Laplace's law.

Introduction of a stress function ψ defined by

$$\psi = rP_H \tag{12}$$

where P_H is the horizontal stress component (Fig. 2) yields, after a lengthy manipulation of equations 7, 8, and 9, a system of differential equations which may be written in the form

$$\begin{aligned} &a_{11}\beta'' + a_{12}\beta' \cot \xi + (a_{13} + a_{14} \cot^2 \xi)\beta \\ &+ a_{15}\psi'' + a_{16}\psi' \cot \xi + (a_{17} + a_{18} \cot^2 \xi)\psi \\ &= pF_1 \sin \xi \cos \xi \end{aligned} \tag{13}$$

$$\begin{aligned} &b_{11}\beta'' + b_{12}\beta' \cot \xi + (b_{13} + b_{14} \cot^2 \xi)\beta \\ &+ b_{15}\psi'' + b_{16}\psi' \cot \xi + (b_{17} + b_{18} \cot^2 \xi)\psi \\ &= pF_2 \sin \xi \cos \xi \end{aligned} \tag{14}$$

where the a_{ij}, b_{ij}, and F_j are functions of ξ and the geometry of the left ventricle. Since simplified expressions are to be obtained for the solutions to equations 13 and 14, the lengthy expressions for these quantities a_{ij}, etc., will not be detailed here. One can show however, that for thin shells these equations reduce to the system developed by Clark and Reissner (1957) in their studies of thin ellipsoidal shells under internal pressure.

Solutions to the Equations of Equilibrium

Two methods are employed for the solutions to the differential equations 13 and 14. The first method involves a Runga-Kutta procedure and yields a more accurate picture of the stress field over the entire myocardium. This procedure follows closely the work of Galletly et al. (1961) and discussed in more detail by Mirsky and Sallin (1968) and therefore will not be repeated in this analysis.

Although the numerical integration solution is more accurate over the entire myocardium it has several disadvantages in that (*a*) machine calculations are expensive and (*b*) calculations must procede in a stepwise fashion so that if one is interested in equatorial stresses only ($\xi = \pi/2$), one must first perform all intermediate calculations from $\xi = 0$ on. It is therefore of practical interest to obtain an analytical solution to the system of equations 13 and 14 which can be applied directly to the locations of interest.

In their studies of thin ellipsoidal shells subject to internal pressure, Clark and Reissner (1957) obtained solutions to the equations of equilibrium in the form of

asymptotic expansions involving powers of a small parameter. The leading terms of their expansions correspond with the membrane solution and the remaining terms of the series represent corrections to the membrane solution. A similar approach is employed here for the solutions of equations 13 and 14.

The functions β and ψ are expressed in the form

$$\beta = (pb\mu/2Eh) \sum_{n=0}^{\infty} (1/\mu^{n+1}) f_n(\xi)$$

$$\psi = (pb^3/2a) \sum_{n=0}^{\infty} (1/\mu^n) g_n(\xi) \tag{15}$$

where E is Young's modulus for the wall material

$$\mu = (b^2/ah)[12(1 - \nu^2)]^{1/2} = 3b^2/ah \quad \text{for} \quad \nu = 0.5.$$

If we substitute expression 15 into equations 13 and 14 and equate the various powers of μ we obtain the following expressions for the first few terms of the expansions 15.

$$\begin{aligned}
g_0(\xi) &= \sin \xi \cos \xi \\
f_0(\xi) &= (b/\alpha a^2)(b^2 - a^2)[3 + (b/\alpha)^2] \sin \xi \cos \xi \\
g_1(\xi) &= -3(b/\alpha) \sin \xi \cos \xi \\
f_1(\xi) &= 0 \\
g_2(\xi) &= (b/a)^4(b^2 - a^2)^3[(1.125/\alpha^6) + 1.875(b^2/\alpha^8)] \sin^3 2\xi \\
&\quad + (b/a)^4(b^2 - a^2)^2[(2.25/\alpha^4) + 2.25(b^2/\alpha^6)] \sin 4\xi \\
&\quad + [(b/a)^4(b^2 - a^2)\{-(4.5/\alpha^2) - 1.5(b^2/\alpha^4) + (b^4/\alpha^6) \\
&\quad - 2.25(a^2b^2/\alpha^6) - 1.5(a^2b^4/\alpha^8) - 2.625(a^2/\alpha^4)\} \\
&\quad + 2.25(b/\alpha)^2 - 1.125(b^4/\alpha^2a^2)] \sin 2\xi \qquad (16) \\
&\quad \text{etc.}
\end{aligned}$$

For the present analysis the expansions for β and ψ are approximated by

$$\psi \sim (pb^3/2a)\left[g_0(\xi) + \frac{1}{\mu} g_1(\xi) + \frac{1}{\mu^2} g_2(\xi)\right]$$

$$\beta \sim (pb/2Eh) f_0(\xi). \tag{17}$$

Although the functions $f_n(\xi)$ and $g_n(\xi)$ represent only particular solutions of the differential equations, these expansions satisfy the boundary conditions

$$\beta = 0, \qquad \psi = 0 \quad \text{at} \quad \xi = 0, \pi/2 \tag{18}$$

term by term and therefore it is unnecessary to consider the general solution of the homogeneous portion of equations 13 and 14.

In terms of the functions $f_n(\xi)$ and $g_n(\xi)$ the stress and moment resultants may be written as

$$N_{\xi\xi} = (pb^3/2a\alpha)\left[g_0(\xi) + \frac{1}{\mu}g_1(\xi) + \frac{1}{\mu^2}g_2(\xi)\right]\cot\xi$$
$$+ (pab/2\alpha)[1 - (ha/2\alpha b)]^2 \sin^2\xi$$
$$N_{\theta\theta} = (pb^3/2a\alpha)\left[g_0'(\xi) + \frac{1}{\mu^2}g_1'(\xi) + \frac{1}{\mu^2}g_2'(\xi)\right]$$
$$+ (pab/\alpha)[1 - (hab/2\alpha^3)][1 - (ha/2\alpha b)]\sin^2\xi$$
$$M_{\xi\xi}/h^2 = (Eh/9)(\kappa_\xi + 0.5\,\kappa_\theta) + (Eha/9\alpha b)(0.4\epsilon_\xi - 0.7\epsilon_\theta)$$
$$- (Ehab/9\alpha^3)(2.2\epsilon_\xi + 1.1\epsilon_\theta) + pH^-[0.1 + (ha/120\alpha b)$$
$$+ (hab/20\alpha^3)]$$
$$M_{\theta\theta}/h^2 = (Eh/9)(\kappa_\theta + 0.5\kappa_\xi) + (Ehab/9\alpha^3)(0.4\epsilon_\theta - 0.7\epsilon_\xi)$$
$$- (Eha/9\alpha b)(2.2\epsilon_\theta + 1.1\epsilon_\xi)$$
$$+ pH^-[0.1 + (hab/120\alpha^3) + (ha/20\alpha b)] \tag{19}$$

where the quantities κ_ξ, κ_θ, ϵ_ξ, and ϵ_θ are given in the appendix.

Guided by the work of Naghdi (1957), the components of stress as functions of the thickness coordinate ζ are

$$\sigma_{\xi\xi} = [N_{\xi\xi}/h + (12M_{\xi\xi}/h^3)\zeta]/(1 + \zeta a/\alpha b)$$
$$\sigma_{\theta\theta} = [N_{\theta\theta}/h + (12M_{\theta\theta}/h^3)\zeta]/(1 + \zeta ab/\alpha^3). \tag{20}$$

Note that the stresses at the endocardial, middle, and epicardial surfaces are obtained by setting in turn $\zeta = -h/2$, 0, and $h/2$ in the above expressions. In particular, the stresses at the middle surface are given by

$$\sigma_{\xi M} = N_{\xi\xi}/h$$
$$\sigma_{\theta M} = N_{\theta\theta}/h$$
$$\sigma_{\zeta M} = -1.5(ab/h\alpha^3)\left(M_{\xi\xi} + \frac{\alpha^2}{b^2}M_{\theta\theta}\right) - 0.5\,pH^- \tag{21}$$

where the subscripts ξ, θ, and ζ denote the meridional, circumferential, and radial directions, respectively.

Development of Laplace's Law

At this stage of the analysis it is worthwhile examining the zeroth order solution represented by

$$\psi_0 = (pb^3/2a)g_0(\xi) = (pb^3/2a) \sin \xi \cos \xi$$

$$\beta_0 = (pb/2Eh)f_0(\xi)$$

$$= (pb^2/2Eh\alpha a^2)(b^2 - a^2)[3 + (b/\alpha)^2] \sin \xi \cos \xi. \tag{22}$$

For very thin shells $h/b \ll 1$ and the expressions 19 for the stress resultants reduce to

$$N_{\xi\xi} = pb\alpha/2a$$

$$N_{\theta\theta} = (pb\alpha/a)[1 - (b^2/2\alpha^2)] \tag{23}$$

which agree with the results in the text by Timoshenko (1940). If we introduce the principal radii of curvature defined by

$$R_\xi = \alpha^3/ab \qquad R_\theta = \alpha b/a \tag{24}$$

a simple analysis yields the result

$$N_{\xi\xi}/R_\xi + N_{\theta\theta}/R_\theta = p \tag{25}$$

which is one form of the generalized Laplace's law. Furthermore, to this order of approximation and assuming $h/b \ll 1$, the effects due to bending which involve the quantities $M_{\xi\xi}$ and $M_{\theta\theta}$ are negligible.

Simplified Expressions for Equatorial Stresses

In the development of the basic equations of equilibrium, terms of the order $0(h^2)$ were included. Thus for consistency, any simplified expressions obtained from the asymptotic solutions 16 and 19 should include at most, terms of the order $0(h^2)$. As will be noted later in the discussion of the numerical results the maximum stresses occur at the equatorial plane $\xi = \pi/2$. Fortunately this is the region where the asymptotic solution converges more rapidly and is in better agreement with the numerical integration solution.

On carrying out the analysis we find with the aid of expressions 19 and 20 that a simplified version of the equatorial stresses is given in the form

$$\sigma_{\xi\xi} = [\sigma_{\xi ME} + (2\zeta/h)\sigma_{\xi BE}]/(1 + \zeta/b)$$

$$\sigma_{\theta\theta} = [\sigma_{\theta ME} + (2\zeta/h)\sigma_{\theta BE}]/(1 + \zeta b/a^2) \tag{26}$$

where the membrane stresses $\sigma_{\xi ME}$, $\sigma_{\theta ME}$, and the bending stresses $\sigma_{\xi BE}$ and $\sigma_{\theta BE}$ are

$$\sigma_{\xi ME} = (pb/2h)(1 - h/2b)^2$$

$$\sigma\theta_{ME} = (pb/h)(1 - h/2b)(1 - hb/2a^2)$$
$$- (pb^3/2a^2h)[1 - (h/b) + (h^2/9b^2)\{4.5 + 3(b/a)^2$$
$$+ 2.25(b/a)^4 + 2.5(b/a)^6 - 10(b/a)^8\}]$$

$$\sigma_{\xi B} = 6M_{\xi\xi}/h^2$$
$$= (p/4)[1 + 3(b/a)^2 - (8/3)(b/a)^4 - (4/3)(b/a)^6$$
$$- (h/b) + 0.25(h/b)^2 + 0.55(h/a)^2 + 0.9(hb/a^2)^2]$$

$$\sigma_{\theta B} = 6M_{\theta\theta}/h^2$$
$$= -(p/2)[1 - 2.5(b/a)^2 + 1.167(b/a)^4 + 0.333(b/a)^6$$
$$- 0.323(h/b)^2 + 0.23(h/a)^2 + 0.5(hb/a^2)^2$$
$$- 1.42(b^2h^2/a^4)]. \qquad (27)$$

These expressions involve simple algebraic quantities which can be readily adapted to small laboratory-oriented digital computers employed for the clinical evaluation of patient status.

Laplace Formulae for a Prolate Spheroid, Sphere, and General Ellipsoid

There appears to be a great deal of confusion with regard to the application of Laplace's law for the evaluation of ventricular wall stresses. This is not too surprising since the formulae in the classical texts do not explicitly state which geometry should be employed. For a thin shell, the question of whether internal geometry or midwall geometry should be used is academic. However, if one wishes to apply Laplace's law beyond its range of validity i.e. for thick shells, the choice of geometry is very important.

It is of practical interest therefore, to compare the results obtained from the various versions of Laplace's law with those obtained from thick shell theory when available. In particular, we will consider those geometries which are appropriate for the left ventricle namely prolate spheroid, sphere, and general ellipsoid. Obviously one can only compare mean stresses since the basic assumption made in the development of Laplace's law is that the stresses are constant through the thickness. Stresses will be compared in the equatorial region only since this is the location of maximum stresses. In an attempt to assess the geometrical assumption

of a prolate spheroid, comparisons will be made later in the analysis with results obtained from the formulae for a general ellipsoid.

Prolate Spheroid. The generalized form of Laplace's law for a prolate spheroid may be written as

$$\sigma_{\xi\xi}/R_\xi + \sigma_{\theta\theta}/R_\theta = p/h \tag{28}$$

where the quantities have been previously defined. If we assume that the radii of curvature R_ξ and R_θ refer to the endocardial surface, then at the equator

$$R_\xi = a_i^2/b_i, \qquad R_\theta = b_i \tag{29}$$

where a_i and b_i are, respectively, the semimajor and semiminor axes of the internal elliptical cross-section.

At the equator, the meridional mean stress $\sigma_{\xi\xi}$ is obtained directly by equilibrating the forces to the pressure loading p with the result

$$\sigma_{\xi 1}\pi[(b_i + h)^2 - b_i^2] = p\pi b_i^2$$

or

$$\sigma_{\xi 1} = pb_i^2/(2b_i + h)h \tag{30}$$

and the corresponding circumferential stress $\sigma_{\theta\theta}$ is given by

$$\sigma_{\theta 1} = (pb_i/h)[1 - b_i(b_i/a_i)^2/(2b_i + h)]. \tag{31}$$

If we assume midwall geometry for the radii of curvature, the resulting expressions as obtained from equation 23 are

$$\sigma_{\xi 2} = pb/2h$$

$$\sigma_{\theta 2} = (pb/h)[1 - (b^2/2a^2)]. \tag{32}$$

Sphere. For a sphere the meridional and circumferential stresses are equal and independent of the angular coordinates. If we equilibrate forces at the equator we obtain as before the result

$$\sigma_{\theta 3} = \sigma_{\xi 3} = pb_i^2/h(2b_i + h). \tag{33}$$

Alternatively by direct application of Laplace's law (equation 28), employing internal geometry and midwall geometry, the stresses are given by

$$\sigma_{\theta 4} = \sigma_{\xi 4} = pb_i/2h \tag{34}$$

$$\sigma_{\theta 5} = \sigma_{\xi 5} = pb/2h \tag{35}$$

where b_i is the internal radius of the sphere and b is the midwall or mean radius. These formulae are to be compared with the exact result for the mean stress namely

$$\sigma_{\theta E} = pb_i(4b_i^2 + b_0^2 + b_ib_0)/4(b_0^3 - b_i^3) \tag{36}$$

where b_0 is the outer radius of the sphere.

General Ellipsoid. Biplane angiocardiography reveals that the assumption of a prolate spheroid (at least in diastole) is a reasonable one for the human left ventricle, however, for the dog a general ellipsoid may be a closer approximation. It is therefore of interest to make a qualitative comparison between the Laplace law for a prolate spheroid and a general ellipsoid.

Flügge (1966) presents formulae for the stresses in a thin general ellipsoid. The stresses are now functions of both the meridional angle φ and the circumferential coordinate θ. At the equator, the expressions for the stresses reduce to

$$\sigma_{\xi G} = (pa_i^2/2h)\left[\frac{c_ib_i}{a_i^2} - \left(\frac{c_i}{b_i} - \frac{b_i}{c_i}\right)\cos 2\theta\right] \Big/ [c_i^2 + (b_i^2 - c_i^2)\cos^2\theta]^{1/2}$$

$$\sigma_{\theta G} = (p/2h)\left[\frac{c_i}{b_i} + \frac{b_i}{c_i} - \frac{b_ic_i}{a_i^2}\right][c_i^2 + (b_i^2 - c_i^2)\cos^2\theta]^{1/2} \tag{37}$$

where a_i, b_i, c_i are, respectively, the internal semi-axes in the z, y, and x directions. For the special case of the prolate spheroid ($c_i = b_i$) and the above expressions reduce to

$$\sigma_{\xi p} = pb_i/2h$$

$$\sigma_{\theta p} = (pb_i/h)[1 - b_i^2/2a_i^2] \tag{38}$$

which are consistent with the Laplace formula (equation 28) when internal geometry is employed.

A simple analysis reveals that the maximum hoop stress $\sigma_{\theta G}$ can occur at $\theta = 0$ or $\theta = \pi/2$ depending on the conditions $b > c$ or $b < c$. Since expressions 37 and 38 apply to thin shells only and a thick shell theory is not available for a general ellipsoid one can only make qualitative statements with regard to the effects of the geometry on stresses.

NUMERICAL RESULTS AND DISCUSSION

The expressions 20, 21, and 26 for the circumferential, meridional, and transverse normal stress components have been evaluated throughout the cardiac cycle from data made available through biplane angiocardiography. Average values obtained from $a - p$ and lateral films were assumed for the semiminor axis b. Based on the assumption of incompressibility i.e. constant wall volume, it was possible to obtain wall thicknesses throughout the cardiac cycle even though thicknesses were meas-

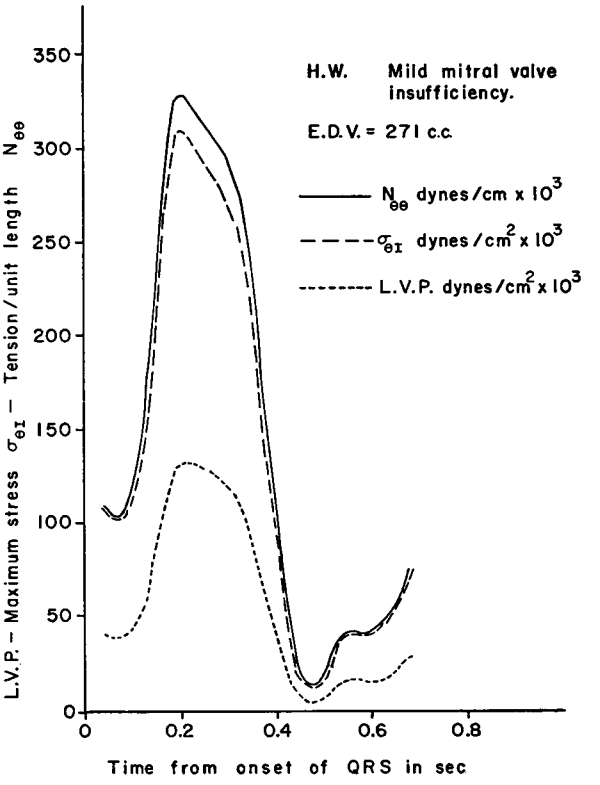

FIGURE 3 L. V. P. (left ventricular pressure), circumferential stress and tension/unit length vs. time.

ured at only several instances during the cycle. Intraventricular pressure data employed, were recorded continuously and simultaneously with the recording of the geometrical data.

In Figs. 3 and 4 the time histories of two patients H.W. and W.E.R. are plotted for the maximum circumferential stress $\sigma_{\theta I}$, the circumferential force/unit length $N_{\theta\theta}$, and the left ventricular pressure p. The maximum stress $\sigma_{\theta I}$ occurs on the endocardial surface at the equator either prior to, or at the time of, peak intraventricular pressure. This result emphasizes the importance and dependence of stress not only on the pressure but in addition, on the changing geometry of the left ventricle particularly during systole. The small oscillations that appear in Fig. 4 and quite often in other ventricular pressure recordings are not always due to poor manometry, but may be indicative of a particular heart disease.

Fig. 5 indicates the variation of midwall stresses and endocardial stresses as we proceed from the apex ($\xi = 0$) to the equator $\xi = \pi/2$. The circumferential stress $\sigma_{\theta I}$ varies only slightly with the angle ξ, however there are marked variations in the meridional stress $\sigma_{\xi I}$ due to the changes in sign of the bending stresses from $\xi = 0$

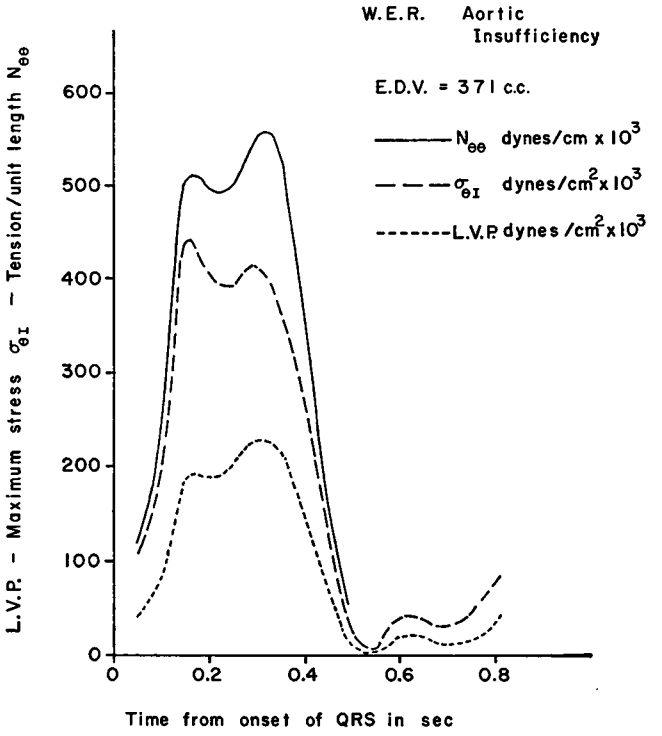

FIGURE 4 L. V. P., circumferential stress and tension/unit length vs. time.

to $\xi = \pi/2$. Stress distribution through the wall thickness are plotted in Fig. 6 for several values of ξ at the time of maximum stress for patient W.E.R. The stress gradients increase as we proceed from the equator to the apex where bending stresses become more significant. In general, the stresses decrease from a maximum value on the endocardial surface to a minimum on the epicardial surface. It should be noted further that the circumferential and meridional stresses are positive (tensile) but the radial stress $\sigma_{\xi\xi}$ is always negative (compressive). The radial stress on the endocardial surface which corresponds to the intraventricular pressure is approximately 40% of the maximum stress developed and therefore must be included in an analysis of thick shells. In the development of Laplace's law this stress is neglected entirely.

The curves depicted in Figs. 3–6 have been evaluated on the basis of the numerical integration solution. As stated previously this solution yields more accurate values for the stresses over the entire range of ξ. However, the numerical integration procedure requires a large computer of the order of the IBM 7094 for the evaluation of the stresses. Fortunately, the asymptotic solution which is valid near the equator $\xi = \pi/2$ produces rapid results for the maximum stresses in agreement with the numerical integration solution. These equatorial stresses furthermore, agree

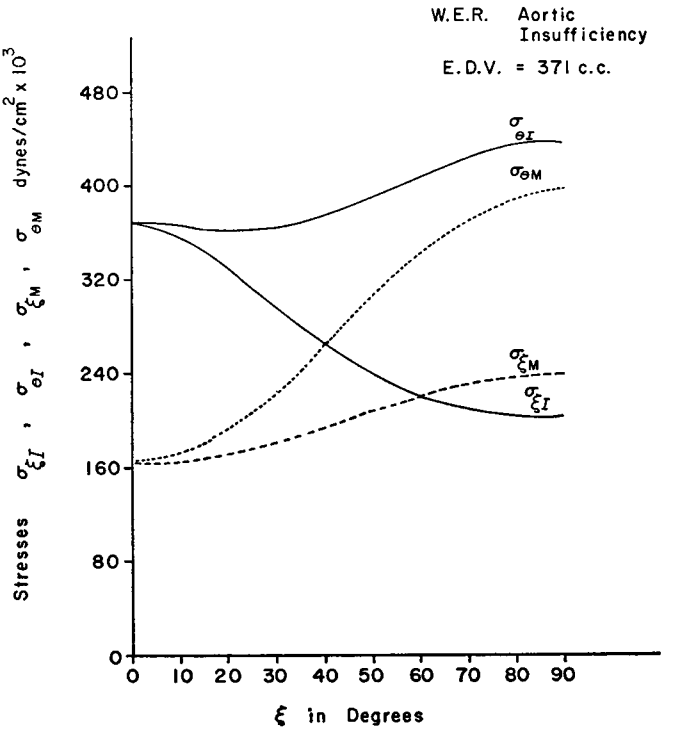

FIGURE 5 Variation of stresses with ξ for patient W. E. R.

with the results obtained by Wong and Rautaharju (1968). This result is not too surprising since the effects of bending stresses, which were neglected in their analysis, are insignificant at the equator $\xi = \pi/2$.

The present theory is compared with a known exact solution for the special case of the sphere ($b = a$). Table I indicates the comparison of the maximum stress $\sigma_{\theta I}$ for various h/b ratios and the discrepancy is observed to be less than 6% for $h/b = 0.5$ which is generally the highest ratio encountered in a cardiac cycle for the left ventricle. For the average stresses the present theory and exact theory are essentially identical. The striking result of Table I however, is the close agreement between the exact theory and a "modified Laplace's law" given by expression 33 for $\sigma_{\theta 3}$. Formulae 34 and 35 which are obtained from Laplace's law based on internal and midwall geometry are in error by 40–100% for thick shells and should not be employed in estimating mean stresses in thick walled spheres.

In Fig. 7 we observe the comparison of the meridional and circumferential average stresses in a prolate spheroid obtained from the present theory ($\sigma_{\xi ME}$ and $\sigma_{\theta ME}$) with those evaluated on the basis of two versions of Laplace's law ($\sigma_{\xi 1}$, $\sigma_{\theta 1}$ and $\sigma_{\xi 2}$, $\sigma_{\theta 2}$). It is quite evident that the modified form of Laplace's law based on internal geometry and given by formulae 30 and 31 are in closer agreement with

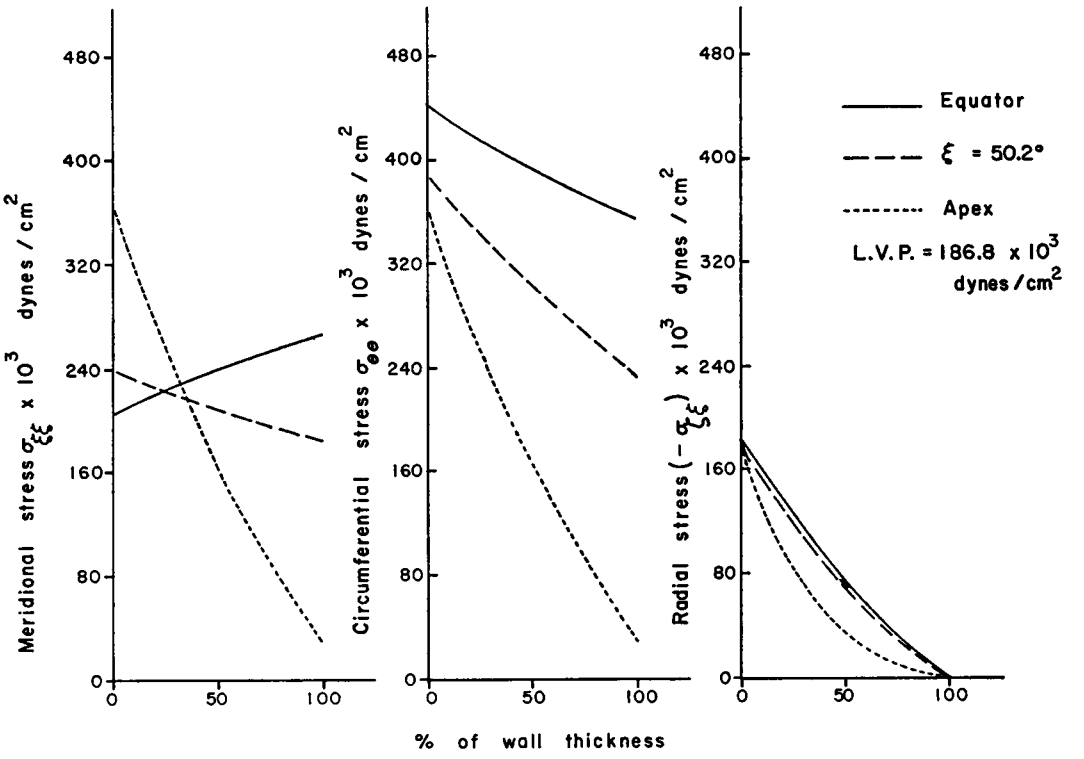

FIGURE 6 Stress distribution through wall at various values of ξ for patient W. E. R.

TABLE I

COMPARISON OF PRESENT THEORY AND LAPLACE'S LAW WITH EXACT SOLUTION FOR A SPHERE

h/b	Maximum stress $\sigma_{\theta I}/p$		Average stresses				
			Exact	Present	Laplace		
	Exact	Present			$\sigma_{\theta 3}/p$	$\sigma_{\theta 4}/p$	$\sigma_{\theta 5}/p$
0.1	4.78	4.77	4.51	4.51	4.51	4.75	5.25
0.2	2.35	2.30	2.07	2.03	2.03	2.25	2.75
0.3	1.52	1.49	1.22	1.21	1.20	1.42	1.92
0.4	1.13	1.09	0.81	0.82	0.80	1.00	1.50
0.5	0.91	0.86	0.59	0.58	0.56	0.75	1.25

the present thick-wall theory. The meridional stresses are actually identical and the circumferential mean stresses differ by no more than 15% from the present theory for relatively thick shells ($h/b = 0.5$). Thus Laplace's law as given by $\sigma_{\xi 1}$ and $\sigma_{\theta 1}$ is a useful and reasonably accurate formula for calculating average ventricular wall stresses.

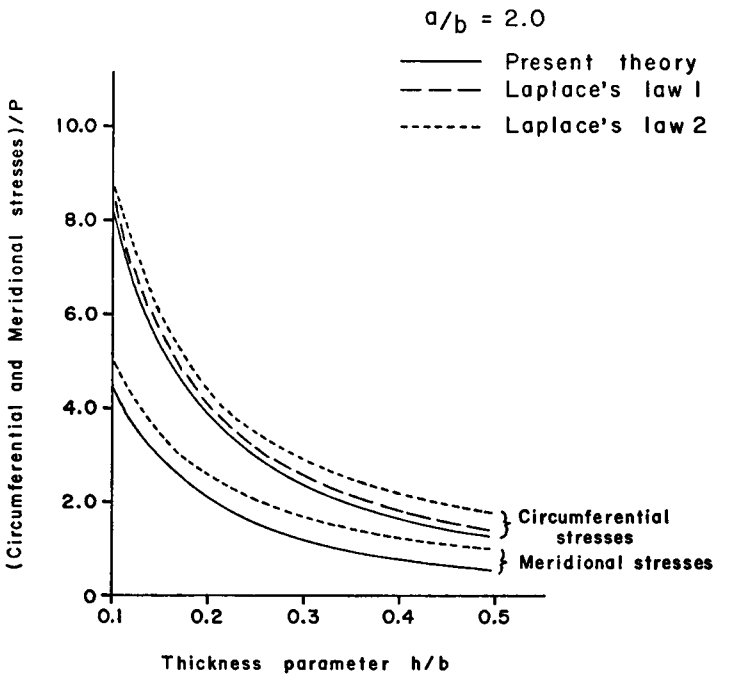

FIGURE 7 Comparison of Laplace's law with the present theory.

If semiminor axes differ by 30% a comparison of formulae 37 and 38 indicate that stresses in a general ellipsoid may be 25% higher than those in a prolate spheroid where the minor axis is taken to be the average of the two minor axes of the general ellipsoid. According to Sandler,[1] the dog heart more closely approximates the general ellipsoid and therefore one should be cautious in extrapolating data from dog to human as is so often done. Fortunately, human data as recorded by biplane angiocardiography rarely reveal such large discrepancies between the lateral and a $-p$ semiminor axes.

We are now in a position to assess the validity of the restrictive assumptions made in the present thick shell theory. Over the past three decades a number of experimental studies have been performed in relation to the intramyocardial pressure distribution. Johnson and DiPalma (1939) noted that during the height of systole there exists in the left ventricular wall a gradient of pressure decreasing from the deeper to the more superficial layers. Similar results were obtained in the studies by Laszt and Müller (1958) and Kreuzer and Schoeppe (1963). In fact Kreuzer and Schoeppe showed that the maximum intramyocardial pressure exceeded the maximum left ventricular pressure and occurs in the inner layers near the endocardial surface. Furthermore, the myocardial pressure decreases to zero at the outer surface

[1] Sandler, Harold. Private communication.

and to the level of the intraventricular pressure at the inner surface of the ventricular wall. Qualitatively, these results are in agreement with those predicted by the present theory and shown plotted in Fig. 6 except that the theoretical results always predict a maximum at the endocardial surface. There is a danger however in attempting to carry too far the comparison between theory and experiment. In most of the experimental investigations a fluid pressure is being measured in which case all three components of stress $\sigma_{\theta\theta}$, $\sigma_{\xi\xi}$, and $\sigma_{\zeta\zeta}$ are equal. This result certainly cannot be predicted by the present theory. Kirk and Honig (1964) who also studied intramyocardial pressures admit that they were not always sure of the "pressures" they were recording.

A further validation of the theory in part is suggested by the work of Spotnitz et al. (1966) in their studies of sarcomere structure relative to pressure volume curves of intact left ventricles of dog and cat. Their studies have shown that at given ventricular filling pressures the sarcomeres are longest in the inner layers of the myocardium decreasing in length towards the epicardial surface. These results suggest that the stresses are maximum at the inner layers and minimum at the epicardial surface.

The assumption of a prolate spheroid throughout the cardiac cycle may be restrictive during systole since infoldings and crenations have been observed with castings and filming of steel markers attached to the endocardial surface. These factors could introduce errors in the evaluation of wall thickness and also account for a maximum stress occurring within the myocardial wall. Furthermore, the theory presented here has been developed for the mechanical behavior of the myocardium as passive biomatter and strictly speaking is not valid for the systolic phase of the cardiac cycle. It may well be that the assumptions of isotropy and homogeneity are reasonable for diastole but for systole the effects of anisotropy and nonhomogeneity must be included. For an isotropic material the stresses depend on the pressure and geometry, however with anisotropy included, the elastic constants become additional independent variables.

Although the present theory has its limitations, recent results obtained by Hugenholtz et al. (1968) have indicated that myocardial muscle performance can be accurately assessed from force-velocity relations applying this thick wall theory during systole. Certainly one may be on firmer ground applying this theory for the evaluation of a modulus via an analysis of the third heart sound which occurs during diastole. Until more sophisticated experiments can be performed, it appears that more complex mathematical models which include nonhomogeneity, anisotropy, and large deformations will yield qualitative information only. Thus for the present one may regard this theory as being the next best approximation after Laplace's law.

The author is indebted to Dr. Harold T. Dodge and one of his associates Morris Frimer for furnishing the biplane data, to Richard A. Waterhouse for his assistance in the numerical analysis, and to Mrs. Sallie R. Ames for typing the manuscript.

This work was supported by a grant from the USPHS, GM-14938-01-6458-2 and GRSG, 5-S01 FR-05489-069971-2.

Received for publication 21 July 1968.

APPENDIX

Expressions for strain quantities $\varkappa_\xi$, $\varkappa_\theta$, ϵ_ξ, and ϵ_θ.

The midwall strains ϵ_ξ and ϵ_θ and the quantities $\varkappa_\xi$ and $\varkappa_\theta$ which appear in the expressions 19; for the moment resultants are given by

$$E\epsilon_\xi = E[(u_\xi'/\alpha) + (w_\xi/R_\xi)]$$

$$= (N_{\xi\xi} - 0.5N_{\theta\theta})/h + (Eh^2ab/36\alpha^3)(7.5\kappa_\xi + 4.5\varkappa_\theta)$$

$$- (Eh^2a/12\alpha b)\varkappa_\xi + (pH^-/4)[1 + (ha/3\alpha b) - (4hab/15\alpha^3)]$$

$$E\epsilon_\theta = E[(r'u_\xi/\alpha r) + (w_\xi/R_\theta)]$$

$$= (N_{\theta\theta} - 0.5N_{\xi\xi})/h + (Eh^2a/36\alpha b)(4.5\varkappa_\xi + 7.5\varkappa_\theta)$$

$$- (Eh^2ab/12\alpha^3)\varkappa_\theta + (pH^-/4)[1 + (hab/3\alpha^3) - (4ha/15\alpha b)]$$

$$E\varkappa_\xi = E\beta'/\alpha = (pb/2h\alpha)f_0'(\xi)$$

$$E\varkappa_\theta = (E\beta/\alpha)\cot\xi = (pb/2h\alpha)f_0(\xi)\cot\zeta$$

where

$$H^- = [1 - (hab/2\alpha^3)][1 - (ha/2\alpha b)].$$

REFERENCES

BURCH, G. E., C. T. RAY, and J. A. CRONVICK. 1952. *Circulation.* **5**:504.

BURTON, A. C., 1957. *Amer. Heart J.* **54**:801.

CLARK, R. A. and E. REISSNER. 1957. *J. Mech. Phys. Solids.* **6**:63.

FLÜGGE, WILHELM. 1966. Stresses in Shells. Springer-Verlag, New York Inc.

GALLETLY, G. D., W. T. KYNER, and E. E. MOLLER. 1961. *J. Soc. Ind. Appl. Math.* **9**:489.

GHISTA, DHANJOO N., and HAROLD SANDLER. 1967. An analytical model for the shape and the forces in the left ventricle. N.A.S.A. Ames Research Centre, Moffett Field, Calif.

HUGENHOLTZ, PAUL, I. MIRSKY, CHARLES URSCHEL, HAROLD SANDLER, EDWARD KAPLAN, and EDMUND H. SONNENBLICK. 1968. V_{MAX} and myocardial force-velocity relations: A useful and sensitive measure of contractility in man. Submitted for publication.

JOHNSON, J. RAYMOND, and JOSEPH R. DIPALMA. 1939. *Amer. J. Physiol.* **125**:234.

KIRK, EDWARD S., and CARL R. HONIG. 1964. *Amer. J. Physiol.* **207**:361.

KREUZER, H., and W. SCHOEPPE. 1963. *Arch. Ges. Physiol.* **278**:181.

LASZT, L., and A. MÜLLER. 1958. *Helv. Physiol. Pharmacol. Acta.* **15**:38.

MIRSKY, I. 1964. *J. Acoust. Soc. Amer.* **36**:41.

MIRSKY, I. 1967. A mathematical theory for the mechanics of the myocardium. Part 1. Formulation of the stress differential equations of equilibrium. Division of Mathematical Biology, Dept. of Medicine, Harvard Medical School and Peter Bent Brigham Hospital, Boston, Mass. Interdepartmental report.

MIRSKY, I., and EDWARD A. SALLIN. 1968. "Numerical Integration method for the evaluation of left ventricular stresses". Department of Medicine, Harvard Medical School, Boston, Mass., and

Department of Biomathematics, Univ. of Alabama Medical Centre, Birmingham, Ala. Interdepartmental report.
NAGHDI, P. M. 1957. *Quart. Appl. Math.* **14**:369.
REISSNER, E. 1950. *J. Math. Phys.* **29**:90.
SANDLER, HAROLD, and HAROLD T. DODGE. 1963. *Circ. Res.* **13**:91.
SPOTNITZ, H. M., E. H. SONNENBLICK, and D. SPIRO. 1966. *Circ. Res.* **18**:49.
TIMOSHENKO, S. 1940. Theory of Plates and Shells. McGraw-Hill Book Company Inc., New York.
WONG, ALAN Y. K. and P. M. RAUTAHARJU. 1968. *Amer. Heart J.* **75**:649.
WOOD, R. N. 1892. *J. Anat. Physiol.* **26**:302.